International Journal of Thermophysics, Vol. 1, No. 2, 1980

Some Thermodynamic Aspects of the High-Temperature Transition in Doped V_2O_3

G. M. Joshi,[1] H. V. Keer,[1,2] and J. M. Honig[1]

Received April 30, 1980

Measurements of the entropy change are reported for the high-temperature metal-insulator (MI) transitions in the $(V_{1-x}Cr_x)_2O_3$ and $(V_{1-x}Al_x)_2O_3$ systems. It is emphasized that the entropy of the I phase exceeds that of the M phase. Evidence is presented to show that the M and I phases coexist over a narrow temperature range. The transformation is attended by enormous hysteresis effects; these indicate that the lattice plays an important role in the transition. The probable role of Cr^{3+} and Al^{3+} as a dopant in the V_2O_3 lattice is briefly discussed. A phase diagram for the dilute V_2O_3-Al_2O_3 alloy system is presented.

KEY WORDS: entropies of transition in V_2O_3 alloys; metal-insulator transition in V_2O_3 alloys; V_2O_3-Cr_2O_3 and V_2O_3-Al_2O_3 alloys; phase diagram for V_2O_3-Al_2O_3 alloys.

1. INTRODUCTION

Interest in the physical properties of Cr-doped V_2O_3 stems from three sizeable electrical transitions that were first reported by McWhan and co-workers [1–4], and which have since then been followed up by a variety of investigators. At low temperatures, $(V_{1-x}Cr_x)_2O_3$ is an antiferromagnetic insulator (AFI). In the temperature range between 150 and 190 K, depending on the value of x, the alloys undergo a first-order transition: for $0 \leq x < 0.018$, a metallic phase (M) is formed. Alloys with $0.005 < x < 0.018$ undergo a second phase change to a paramagnetic insulator (I) over a small temperature range within a 100° interval bracketing room temperature. On further

[1]Department of Chemistry, Purdue University, West Lafayette, Indiana 47907, USA.
[2]Permanent address: Department of Chemistry, Indian Institute of Technology, Bombay 400076, India.

0195-928X/80/0600-0185$03.00/0

heating, these alloys then revert gradually to a second metallic phase (M′), quite similar to M.

An extensive literature has by now built up concerning the alteration of physical properties of V_2O_3 on doping with Cr_2O_3 [5]. The investigations include structural, electrical, and magnetic properties; however, the thermal characteristics do not appear to have been systematically investigated. Preliminary calorimetric studies by Sinha et al. [6] indicated only a very small enthalpy change (<100 J/mol) in the high-temperature (HT) transition (M-I or α-β transformation) for powdered $(V_{0.99}Cr_{0.01})_2O_3$ single crystals. Later heat capacity (C_p) measurements by Keer et al. [7] showed that the average enthalpy of transitions for $(V_{0.99}Cr_{0.01})_2O_3$ and for $(V_{0.99}Al_{0.01})_2O_3$ fell in the range ~250–330 J/mol of alloy for single crystal needles or platelets. This value fluctuated with the state of subdivision and thermal treatment of the specimens. Subsequently, Kuwamoto et al. [8] and Keer et al. [9] reported on the C_p behavior of $(V_{1-x}M_x)_2O_3$ systems with M = Cr, Al, and $0 \leq x \leq 0.12$. These studies were directed primarily at the low-temperature (LT) transition occurring in the range 150–190 K. These workers reported only briefly on the HT anomaly for compositions with $x = 0.01$, which coincided with the electrical anomaly established earlier.

Since detailed studies on the electrical resistivity of both the Cr- and Al-doped V_2O_3 systems in the HT transition region have now become available [10–13], it seemed of interest to carry out comparable investigations on the enthalpy and entropy of the HT transition in these alloys. Such data are presented below and should assist in determining the relative merits of the various theories that have been proposed to account for the HT transition. Further, in conjunction with heat capacity [7–9], electrical resistivity, and Seebeck coefficient measurements [11, 14] these data have been utilized to construct a phase diagram for the $(V_{1-x}Al_x)_2O_3$ system. As far as the authors are aware, such a phase diagram has not been reported so far.

2. EXPERIMENTAL

Single crystals of Cr- and Al-doped V_2O_3 were grown by the procedure described by Joshi et al. [11]. X-ray powder diffractograms were recorded at room temperature using CuK_α radiation filtered through Ni; the lattice parameters were compared with those reported earlier [11, 14]. The sample stoichiometry was ascertained by reoxidation to V_2O_5 in an atmosphere of oxygen at 670°C, following the procedure adopted by Kuwamoto [12]. The homogeneity of the Cr- or Al-doped crystals was confirmed by scanning electron microscopy. Heat capacities were measured on single crystal needles or plates cut from a boule, using a differential scanning calorimeter (DSC-2) and sapphire as the standard. A scanning rate of 1.25°/min or 10°/min was employed.

3. RESULTS AND DISCUSSION

The relevant data have been summarized in Figs. 1–8.

We first consider a set of recent measurements carried out at a low scanning rate (1.25°/min) on high-quality single crystals. In Fig. 1 are shown the electrical and thermal characteristics [10] of the HT transitions in $(V_{0.99}Cr_{0.01})_2O_3$. It is seen that the electrical resistivity (ρ) transition consists

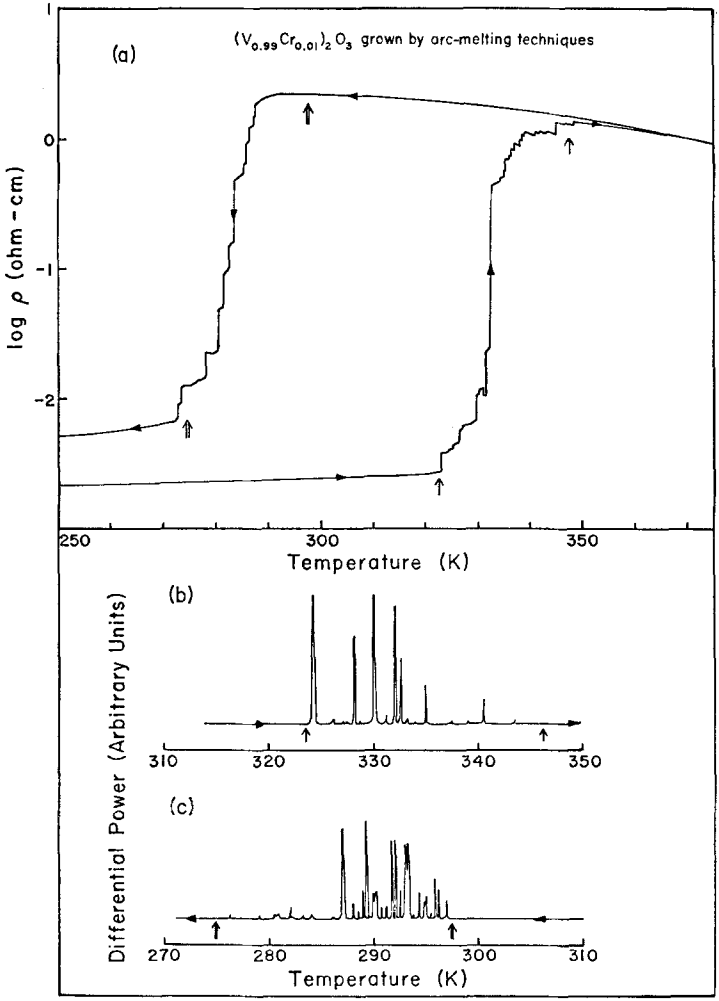

Fig. 1. Electrical resistivity and thermal response of single-crystal $(V_{0.99}Cr_{0.01})_2O_3$ in the region of the high-temperature transition. The very large hysteresis, the discontinuities in resistivity, and the thermal spikes are noteworthy.

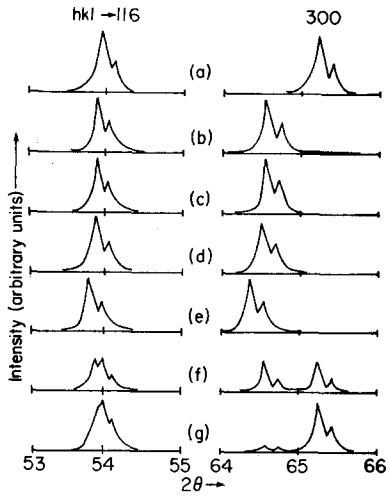

Fig. 2. Changes in the profile of the 116 and 300 Bragg diffraction peaks with temperature: (a) T = 298 K, a = 4.95 Å, c = 14.00 Å; (b) T = 348 K, a = 5.00 Å, c = 13.93 Å; (c) T = 370 K, a = 5.00 Å, c = 13.93 Å; (d) T = 573 K, a = 5.00 Å, c = 13.93 Å; (e) T = 718 K, a = 5.01 Å, c = 13.94 Å; (f) T = 323 K (cooling, biphasic); (g) T = 298 K (cooling, biphasic).

of a series of abrupt jumps in ρ and is accompanied by very large hysteresis effects ($\geq$50 K). Correspondingly, discrete spikes were observed in the DSC scans, obtained at the same scanning rate (1.25°/min). These spikes occur exactly in the same range as the temperature span of the resistivity anomaly. The transition temperature range was always found to be relatively narrow (~15–20 K), although earlier x-ray studies [2, 15] had indicated that the α-β transformation range extended over 150–200 K. Extensive and very accurate crystallographic investigations on pure and Cr-doped V_2O_3 were subsequently carried out by Robinson and coworkers [16–19] above and below the transition, but no attempt was made in these studies to follow the α-β transformation directly. Therefore, we recorded X-ray diffractograms on a 1% Cr-doped V_2O_3 sample, which was grown in a Tri-arc furnace and then precooled to ~210 K to ensure complete conversion to the α-phase. The crystal was then subjected to crystallographic studies in a flowing inert gas atmosphere at regular temperature intervals in the range 300–720 K. Results are displayed in Fig. 2 as the change in profile of the 116 and 300 diffraction peaks with temperature.

Inspection of Fig. 2 shows that the HT transition commences at temperatures higher than 298 K and is completed at temperatures lower than 348 K, indicating that the temperature span of the transition is indeed realtively narrow, in agreement with the findings from heat capacity, resistivity, and thermoelectric studies. The reasons for the discrepancy between the present x-ray data and the earlier studies [2, 15] are not clear; however, subtle deviations from stoichiometry or inhomogeneities in dopant distribution are known to broaden the HT transition range

In a few investigations on Cr- and Al-doped V_2O_3, the electrical

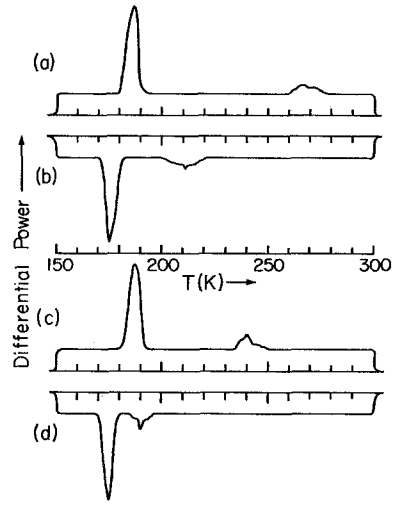

Fig. 3. DSC scans for $(V_{0.986}Cr_{0.014})_2O_3$ during (a) a heating and (b) a cooling cycle and for $(V_{0.985}Al_{0.015})_2O_3$ during (c) a heating and (d) a cooling cycle. The larger and smaller peaks are associated with the LT and HT transitions, respectively. Note the differences in hysteresis effects in the two transformations.

transition occurred essentially in one step, and only 2–4 spikes were then encountered in the DSC scans. These facts strongly suggest that in the ideal case, the transformation might take place at a single temperature in one step.

3.1. Thermodynamic Properties

In order to determine the enthalpy (ΔH) and entropy (ΔS) of transition, a more rapid scanning rate of 10°/min was usually employed. Figure 3 displays typical DSC scans for $(V_{0.986}Cr_{0.014})_2O_3$ and $(V_{0.985}Al_{0.015})_2O_3$. The larger (smaller) peaks are associated with the LT (HT) transformation; one should note the lack of symmetry and the structure in the HT peaks as compared to the LT peaks. Thus the discrete spikes obtained at the slower scanning rate are now broadened into an irregularly shaped pattern, consisting principally of two or more closely spaced peaks of differing heights.

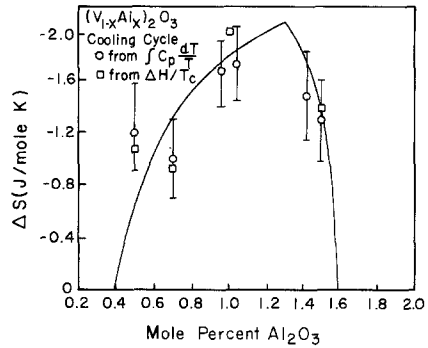

Fig. 4. Plot of the entropy change associated with the high-temperature transition versus x for $(V_{1-x}Al_x)_2O_3$; cooling cycle.

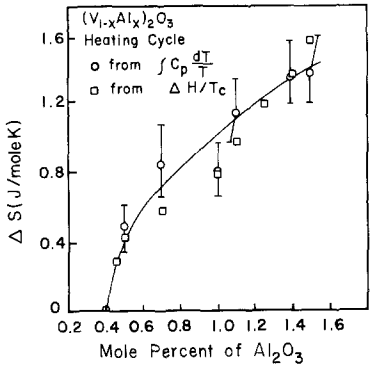

Fig. 5. Plot of the entropy change associated with the high-temperature transition versus x for $(V_{1-x}Al_x)_2O_3$; heating cycle.

However, occasionally a single symmetrical peak was also encountered, and the corresponding resistivity anomaly then consisted of a single, sharp jump.

Results obtained from the fast-scan DSC measurements are displayed in Figs. 4–7 as entropy changes per mole of $(V_{1-x}M_x)_2O_3$ versus x, where M = Al, Cr. Circles represent ΔS values obtained through heat capacity measurements by the standard relation $\Delta S = \int (C_p/T)dT$. Squares represent ΔS values based on enthalpies of transition, which were determined by comparing the area under the differential power curves for the alloys against known standards; here it was assumed that the transition was of first-order. Unfortunately, the scatter in the experimental data is severe; nevertheless, the following points emerge:

1. The compositions over which the HT transition could be discerned by the calorimetric technique extend over the range $0.004 < x < 0.016$ for M = Al and $0.005 < x < 0.018$ for M = Cr, respectively; these

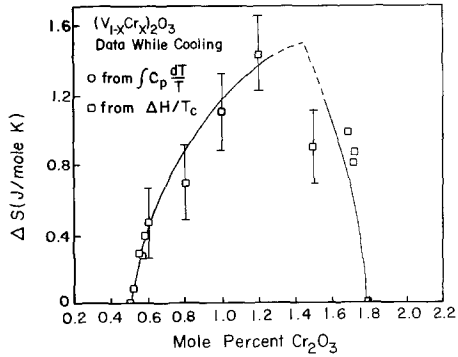

Fig. 6. Plot of the entropy change associated with the high-temperature transition versus x for $(V_{1-x}Cr_x)_2O_3$; cooling cycle.

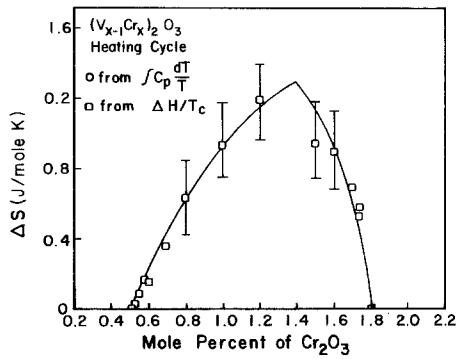

Fig. 7. Plot of the entropy change associated with the high-temperature transition versus x for $(V_{1-x}Cr_x)_2O_3$; heating cycle.

values are in excellent agreement with the ranges determined in all prior electrical resistivity measurements.

2. The entropy changes are positive during the heating and negative during the cooling cycles. These findings are consistent with earlier reports [7, 10] that the entropy of the I phase is greater than that of the M phase. These findings must also be examined in the context of recent Raman studies [20], which show unequivocally that the various Raman-active phonon frequencies in the metallic phase of $(V_{0.985}Cr_{0.015})_2O_3$ lie below those of the I and AFI phases. Thus changes in the contribution to the total entropy by these vibrational degrees of freedom are oppositely directed to those of the electronic

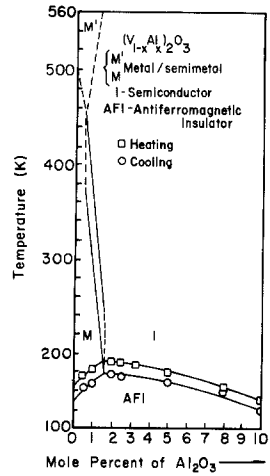

Fig. 8. Phase diagram for the $(V_{1-x}Al_x)_2O_3$ system; it shows a similarity to the corresponding diagram for the $(V_{1-x}Cr_x)_2O_3$ system [13]. Solid lines represent first-order transitions; dashed lines represent the midpoints of second-order transitions involving temperature spans of approximately 200 K.

contributions. For the particular alloy $x_{Cr} = 0.015$, a rough, preliminary estimate yields a value of $(S_I\text{-}S_M)_{ph} \approx -1.7$ J/mol K as the phonon contribution. This would require that $(S_I\text{-}S_M)_{el} \approx +2.9$ J/mol K for the electronic contribution, so as to achieve the net observed entropy change of +1.3 J/mol K. For $x_{Cr} < 0.015$, the two contributions would presumably be roughly proportionally smaller and vanish at $x_{Cr} = 0.005$.

3. The ΔS values are numerically larger for the cooling as compared to the heating cycle. In part, this reflects the enormous hysteresis effects mentioned earlier, on account of which $\Delta H/T$ should be larger at lower temperatures. However, the ΔH values themselves tend to be larger for the cooling than for the heating cycles.
4. Closer inspection of Fig. 4 shows that when x_{Al} is decreased from 0.016 toward 0.004, $|\Delta S|$ first increases very rapidly toward a maximum and then falls off more gradually to zero. The trend is still visible, though less marked, in Fig. 5 and in Figs. 6 and 7 for the variation of ΔS with x_{Cr}. These trends lend credence to claims by the Bell Laboratory research group [2, 21] that the M-I transition is headed toward some critical point near $x_{Cr} = 0.005$. In this picture, one would anticipate that the largest changes in thermodynamic variables should occur for the M-I transition near the triple point $x_{Cr} \approx 0.018$, and that $\Delta S \rightarrow 0$ at the other end of the composition range. In this model, the properties of pure V_2O_3 would then correspond to supercritical behabior, as has been asserted in refs. [2] and [21]. On the other hand, if the assertions of Kuwamoto et al. [22] are correct, then a second metallic or quasimetallic phase (M′) would be encountered at higher temperatures, which is separated from the M or I phases by a second-order transition extending over a temperature range of 200 K. In that event, the singularity at $x_{Cr} = 0.005$ would represent a tricritical point. The very large temperature range of the M-M′ or I-M′ transitions preclude any measurement of ΔH by the experimental techniques available to us in the present investigation. However, independent studies [22–24] appear to indicate the presence of a small entropy change accompanying the M-M′ transition in pure V_2O_3, which could not be detected by us.

3.2 Phase Diagram for the Al-Doped V_2O_3 System

Extensive studies are now available for construction of the phase diagram for the $(V_{1-x}Al_x)_2O_3$ system. Figure 8 is based on measurements of heat capacity [7, 8], electrical resistivity [11, 14], and Seebeck coefficient [11, 14]. This phase diagram bears a similarity to that of the $(V_{1-x}Cr_x)_2O_3$ system constructed by McWhan and co-workers [1, 2, 20], by Rubinstein

[25], and by Kuwamoto et al. [12, 13]. In common with these latter diagrams [12, 13], Fig. 8 shows that the HT transition is associated with an enormous hysteresis of approximately 50 K, which is almost independent of x_{Al} in the range $0.004 < x < 0.016$. This feature indicates that the lattice plays a significant role in the transition. Thus theories that ascribe this transformation solely to electron correlation effects cannot properly account for the experimental situation encountered in the HT transition of the $(V_{1-x}M_x)_2O_3$ (M = Al, Cr) systems.

The AFI-I and AFI-M transitions are associated with hysteresis effects in the 5–10 K range; these are more in line with conventional first-order phase transitions. The stability field of the M′ phase is indicated by the dashed lines in Fig. 8, which show approximately the midpoint of the second-order transitions, encompassing a 200 K span separating the M′ from the M and I phases.

It is noteworthy that, as for the Cr_2O_3–V_2O_3 alloys, the molar volumes $\tilde{V}$ of the $(V_{1-x}Al_x)_2O_3$ system ($x < 0.1$) follow the relation $\tilde{V}_I > \tilde{V}_M$; this fact emerges directly from the values of the lattice parameters as determined by X-ray diffraction experiments [11]. As stated earlier, $\tilde{S}_I > \tilde{S}_M$. Hence, according to the Clausius-Clapeyron relation, $dT/dp > 0$. This implies that the T-p-x diagram for the Al-doped V_2O_3 must be qualitatively similar to the corresponding phase diagram published for the Cr-doped V_2O_3 system.

4. CONCLUSION

By now there is ample evidence that the incorporation of Cr or Al into the V_2O_3 host lattice leads to almost identical effects in all the physical properties that have so far been examined, despite the differences in ionic size or electronic configuration of these two dopants. It is difficult to conceive that the d levels of Al participate in bonding in $(V_{1-x}Al_x)_2O_3$ alloys; thus it is plausible to assume that every Al ion substituting for V removes a cation site, to which the charge carriers can have access. This is in consonance with the well-established trend that with increasing x, the metallic phase of $(V_{1-x}Al_x)_2O_3$ is gradually suppressed.

Presumably, similar considerations apply to Cr^{3+} in V_2O_3. The ground state is the ^3F term, which splits into two doubly degenerate states for which $|M_S| = 1/2$ and $|M_S| = 3/2$. To explain the similarity to the case where Al is used as a dopant, it is necessary to postulate that the various ^3F configurations are all energetically situated well below the Fermi level. This is consistent with the concept that the d^3 ground state is energetically very stable. In that event, electrons again do not have access to cation sites occupied by Cr^{3+}; this qualitatively explains why the metallic characteristics are gradually suppressed by doping V_2O_3 with Cr_2O_3.

ACKNOWLEDGMENT

This research was supported by an NSF-MRL grant to Purdue University, DMR 77–23798.

REFERENCES

1. D. B. McWhan, T. M. Rice, and J. P. Remeika, *Phys. Rev. Lett.* **23:**1384 (1969).
2. D. B. McWhan and J. P. Remeika, *Phys. Rev.* **B2:**3734 (1970).
3. A. Jayaraman, D. B. McWhan, J. P. Remeika, and P. D. Dernier, *Phys. Rev.* **B2:**3751 (1970).
4. A. Menth and J. P. Remeika, *Phys. Rev.* **B2:**3756 (1970).
5. J. M. Honig and L. L. Van Zandt, *Ann Rev. Mat. Sci.* **5:**225 (1975).
6. A. P. B. Sinha, G. V. Chandrashekhar, and J. M. Honig, *J. Solid State Chem.* **12:**402 (1974).
7. H. V. Keer, D. L. Dickerson, H. Kuwamoto, H. L. C. Barros, and J. M. Honig, *J. Solid State Chem.* **19:**95 (1976).
8. H. Kuwamoto, D. L. Dickerson, H. V. Keer, and J. M. Honig, *Mat. Res. Bull.* **11:**1301 (1976).
9. H. V. Keer, H. L. C. Barros, D. L. Dickerson, A. T. Barfknecht, and J. M. Honig, *Mat. Res. Bull.* **12:**137 (1977).
10. H. Kuwamoto, H. V. Keer, J. E. Keem, S. A. Shivashankar, L. L. Van Zandt, and J. M. Honig, *J. Phys. (Paris)* **37(C4):**35 (1976).
11. G. M. Joshi, H. V. Keer, H. Kuwamoto, and J. M. Honig, *Indian J. Pure Appl. Phys.* **15:**471 (1977).
12. H. Kuwamoto, thesis, Purdue University, unpublished (May 1978).
13. H. Kuwamoto, J. M. Honig, and J. Appel, *Phys. Rev.* **B22,** in press.
14. G. M. Joshi, thesis, Purdue University, unpublished (May 1980).
15. G. V. Chandrashekhar and A. P. B. Sinha, *Mat. Res. Bull.* **9:**787 (1974).
16. W. R. Robinson, *ACS Symp. Ser.* **5:**16 (1974).
17. W. R. Robinson, *Mat Res. Bull.* **9:**1091 (1974).
18. W. R. Robinson, *Acta Cryst.* **B31:**1153 (1975).
19. C. E. Rice and W. R. Robinson, *Phys. Rev.* **B13:**3655 (1976).
20. C. Tatsuyama and H. Y. Fan, *Phys. Rev.* **B21:**2977 (1980).
21. T. M. Rice and D. B. McWhan, *IBM J. Res. Develop.* **14:**251 (1970).
22. K. Kosuge, *J. Phys. Chem. Solids* **28:**1613 (1967).
23. J. M. D. Coey, H. Roux-Buisson, C. Schlenker, S. Lakkis, and J. Dumas, *Rev. Gén. Therm.* **15:**1013 (1976).
24. J. M. D. Coey, *Physica* **91B:**59 (1977).
25. M. Rubinstein, *Phys. Rev.* **B2:**4731 (1970).